Letter

Distinct Tamm and Shockley surface states on Re(0001) mixed by spin-orbit interaction

Marcel Holtmann [1,*] Peter Krüger,[2] Koji Miyamoto [3] Taichi Okuda [3] Pascal J. Grenz [1]
Shiv Kumar [3] Kenya Shimada [3] and Markus Donath [1,†]

[1]*Physikalisches Institut, Westfälische Wilhelms-Universität Münster, Wilhelm-Klemm-Straße 10, 48149 Münster, Germany*
[2]*Institut für Festkörpertheorie, Westfälische Wilhelms-Universität Münster, Wilhelm-Klemm-Straße 10, 48149 Münster, Germany*
[3]*Hiroshima Synchrotron Radiation Center, Hiroshima University, 2-313 Kagamiyama, Higashi-Hiroshima 739-0046, Japan*

(Received 13 January 2022; revised 15 March 2022; accepted 6 June 2022; published 30 June 2022)

Tamm and Shockley states, these two paradigmatic concepts are used to describe surface states not only in electronic systems but also in photonic and phononic crystals. The Re(0001) surface hosts both types of electronic surface states in neighboring but qualitatively different energy gaps. Interestingly, spin-orbit interaction generates a double W-shaped energy vs $\mathbf{k}_\parallel$ dispersion by mixing both types of states and lifting their spin degeneracy. By combining spin- and angle-resolved photoemission, tight-binding model calculations, as well as density functional theory including the photoemission process, we develop verifiable criteria to distinguish between the two types of surface states and arrive at a consistent picture of the role of spin-orbit interaction in such a scenario.

DOI: 10.1103/PhysRevB.105.L241412

The appearance of surface states is characteristic for semi-infinite crystals caused by the broken symmetry at the surface. Their description for understanding surface properties is a highly noticed and still ongoing research topic in various fields such as electronic surface states [1–6] and surface states in photonic [7–9] and phononic crystals [10]. Theoretically, two paradigmatic concepts have been used to describe electronic surface states: Tamm-type states [11] split off from noticeably localized bulk states as can be derived, e.g., on the basis of tight-binding models, while Shockley-type states [12] appear in hybridization gaps within nearly-free-electron models. As a consequence, Tamm surface states have often been linked to *d*-derived states with rather flat dispersion, while Shockley surface states to *sp*-derived states with considerable $E(\mathbf{k}_\parallel)$ dispersion.

There is a controversy about whether there is a real physical distinction between the two kinds of states because both appear in gaps of the surface-projected bulk band structure (PBS). Has the distinction only historical reasons based on different mathematical approaches, as suggested by Lüth [5]? Other authors notice an important distinction. According to Zak [13], the existence of Shockley states is derived for a bulk-like potential termination at the surface, while a distortion of the potential in the surface region is essential for the existence of Tamm states. Martin [6] pointed out that Shockley states are "based on a transition in the bulk band structure that is a precursor of modern-day topological insulators." Experimentally, the distinction between Tamm and Shockley states remains to be a challenge [9]. Are they influenced differently by external modifications such as adsorbate atoms?

In the virtue of the classification given by Zak [13], we use the terminology of Tamm and Shockley states along the following lines. In order to classify a surface state in a gap of the PBS, we compare the results of a calculation with the self-consistently computed surface potential and the inclusion of structural relaxation effects (*real* surface) with the band structure of a crystal with truncated bulk potential (*ideal* surface) [14]. Surface states of the *real* surface that vanish at the *ideal* surface are called Tamm states. Shockley states, on the other hand, exist in *inverted* band gaps only [6,12] and are only slightly shifted in energy when going from the *real* to the *ideal* surface. We note that Tamm states can exist in both inverted and noninverted gaps [15].

To make things even more complex, spin-dependent interactions may lift the spin degeneracy in surface states: exchange splittings due to exchange interaction in ferromagnets [16–18] and Rashba-type spin splittings with spin-momentum locking due to spin-orbit coupling (SOC) in high-Z materials [19–21]. As a consequence of SOC, hybridization between different states may occur.

In this Letter, we aim at developing verifiable theoretical and experimental criteria to distinguish between the two types of surface states. For this purpose, we use a surface-related band on Re(0001), which appears in the vicinity of the Fermi level [22–26]. We unravel the origin of its distinctive W-shaped $E(\mathbf{k}_\parallel)$ dispersion behavior and its spin texture, experimentally by (spin- and) angle-resolved photoelectron spectroscopy [(S)ARPES] and theoretically by a tight-binding model as well as detailed DFT (density functional theory) calculations. We show that the Re(0001) surface hosts distinct Tamm and Shockley states that are mixed by SOC.

The (S)ARPES measurements were performed at the BL-9B end station of the Hiroshima Synchrotron Radiation Center (HiSOR), while preliminary data (not shown here) had been taken at BL-1. The photoelectrons were excited by *p*-polarized light of $\hbar\omega = 24$ eV, impinging on the sample at an angle of 50° with respect to the lens axis of the electron detector (hemispherical analyzer VG-Scienta R4000).

*marcel.holtmann@uni-muenster.de
†markus.donath@uni-muenster.de

The Rashba spin component was detected by the ESPRESSO machine [27] using a VLEED (very low-energy electron diffraction) -type spin-polarization detector with a Sherman function of $S = 0.28$. The energy resolution for (S)ARPES was 25 (50) meV, and the angle resolution $\leqslant 1^\circ$. During the measurements the sample was kept at $T < 45$ K and the base pressure in the ultrahigh-vacuum (UHV) chamber was $p < 2 \times 10^{-10}$ mbar.

The Re(0001) surface was prepared as described in Ref. [26]. A perfect hcp(0001) surface exhibits threefold symmetry due to the *A*-*B*-type stacking order and mirror planes along the $\overline{\Gamma}\,\overline{\mathrm{M}}$ directions. The (0001) surface of a grown single crystal, however, shows monoatomic step terraces, terminated either by *A* or *B* layers [28]. Since the spot size of the light beam is large compared with the terrace dimensions, this leads to a simultaneous measurement of both surface terminations and a sixfold surface symmetry with indistinguishable $\overline{\Gamma}\,\overline{\mathrm{M}}$ and $\overline{\Gamma}\,\overline{\mathrm{M}}'$ directions.

The electronic structure has been calculated within the local-density approximation [29] of DFT. A basis of Gaussian orbitals is employed together with pseudopotentials that include scalar relativistic corrections and SOC [30,31]. The Re(0001) surface is treated within a supercell approach using slabs with 40 Re layers. Relaxations of the topmost eight layers have been taken into account. Details of the computations and the resulting structural properties are given in Ref. [26] and in the Supplemental Material [32].

We simulate the photoemission process by assuming a plane wave as the final state and compute the dipole transition matrix elements employing the initial states resulting from our DFT calculation. An exponential damping term with a decay length of 1.25 Å has been used to consider the finite escape depth of the outgoing electrons.

ARPES measurements of Re(0001) are shown in Fig. 1. The photoelectron intensity is given on a linear color scale (black-red-yellow) in (a)–(c). Figure 1(a) presents a constant energy contour (CEC) at $E - E_\mathrm{F} = -55$ meV (not symmetrized). The CEC reflects the sixfold symmetry of the surface with intensity asymmetries for positive and negative k_x caused by the symmetry breaking of the incoming light. Figures 1(b) and 1(c) display $E(\mathbf{k}_\parallel)$ dispersions along $\overline{\Gamma}\,\overline{\mathrm{K}}$ and $\overline{\Gamma}\,\overline{\mathrm{M}}$, respectively and (d) shows the second derivative of the data in (c). Close to E_F, five bands are resolved with increasing wave vector [most clearly discerned in (d)]: an almost circular band with two components of unequal intensity (α low and β high), a rather faint band γ with hexagonal warping and higher intensity along $\overline{\Gamma}\,\overline{\mathrm{K}}$, and a doublet of bands (δ and δ') with larger separation along $\overline{\Gamma}\,\overline{\mathrm{M}}$ compared with $\overline{\Gamma}\,\overline{\mathrm{K}}$. ($\alpha$, β may be associated with SS and δ, δ' with SR1 of Ref. [24]. Similar bands, labeled S10, have been found in Ref. [23].)

To interpret the experimental results, we performed DFT calculations including SOC for the Re(0001) surface along the mirror-plane $\overline{\Gamma}\,\overline{\mathrm{M}}$ direction, which are shown in Fig. 2(a). The PBS is presented in golden color, while the brown dots symbolize surface-derived bands with the dot size being proportional to the electron probability density in the first three layers. A W-shaped surface band stands out, which becomes resonant with bulk states above E_F around $\overline{\Gamma}$. Below E_F, the dispersion resembles that of the experimentally measured α, β, and γ bands.

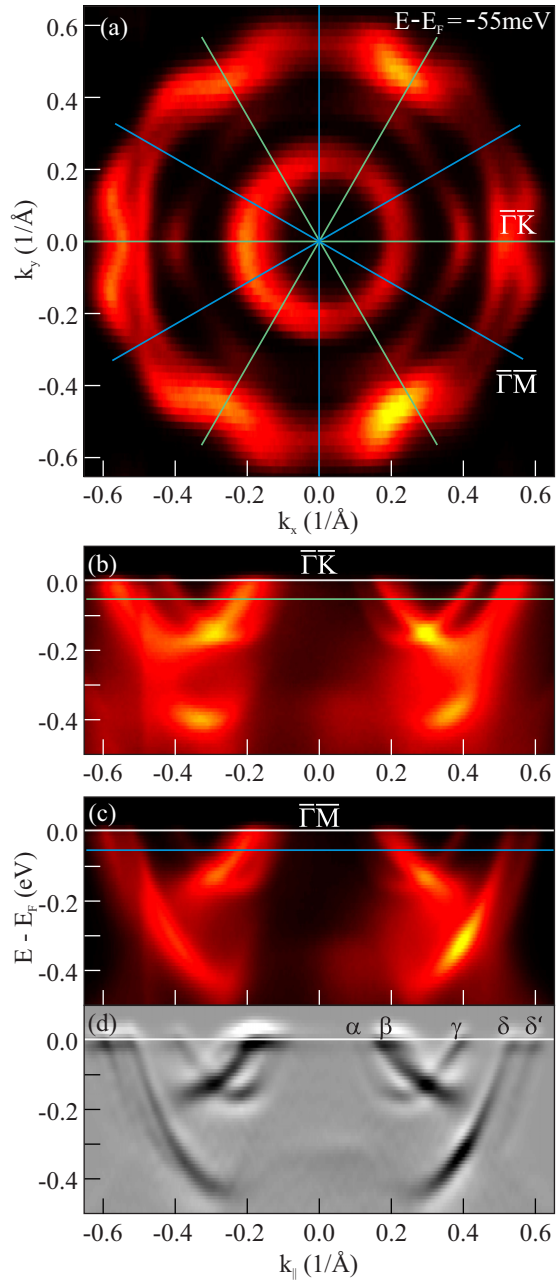

FIG. 1. ARPES data for Re(0001) using light of $\hbar\omega = 24$ eV. (a) Constant energy contour (CEC) at $E - E_\mathrm{F} = -55$ meV. High-symmetry directions $\overline{\Gamma}\,\overline{\mathrm{K}}$ and $\overline{\Gamma}\,\overline{\mathrm{M}}$ are indicated by green and blue lines, respectively. (b),(c) $E(\mathbf{k}_\parallel)$ dispersions along $\overline{\Gamma}\,\overline{\mathrm{K}}$ and $\overline{\Gamma}\,\overline{\mathrm{M}}$. Lines indicate the energy of the CEC in (a). (d) Second derivative of the data along $\overline{\Gamma}\,\overline{\mathrm{M}}$ in (c).

To reveal the origin of these surface bands, we consider DFT results for the *real* surface, yet without SOC. The $\overline{\Gamma}\,\overline{\mathrm{M}}$ direction is, in our coordinate system, along a (y-z) mirror plane of the Re(0001) surface and thus the eigenstates will be either *even* or *odd* with respect to the interchange of x and $-x$. In the case of even states, we observe a surface state in the band gap for $|k_\parallel| \leqslant 0.48$ Å^{-1} [beige colored area in Fig. 2(b)]. The state (including its resonant part) vanishes in a calculation for the *ideal* surface (see Supplemental Material), and thus, we consider it as a Tamm-type state. For odd symmetry, we find a

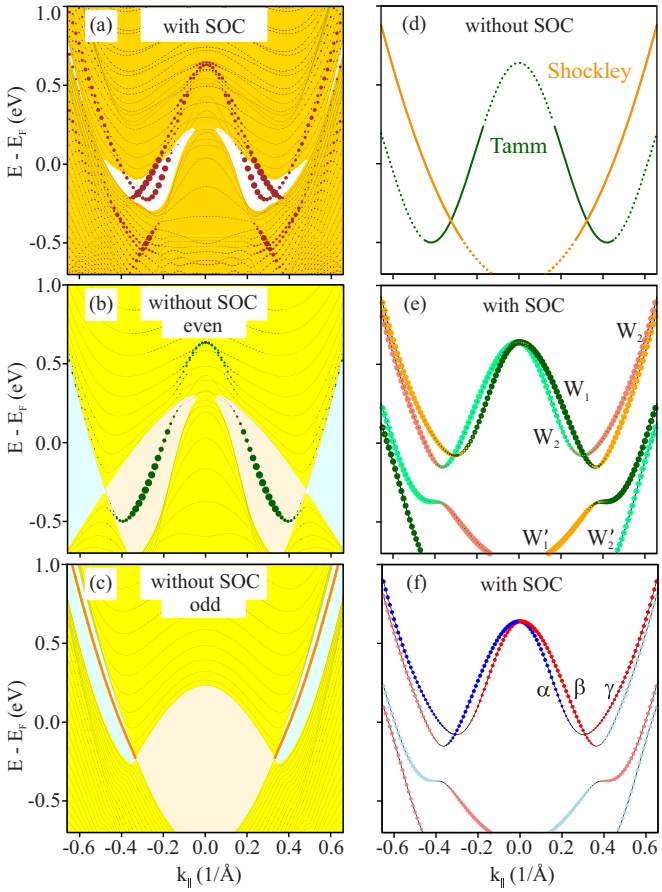

FIG. 2. Band structure of Re(0001) along $\overline{\Gamma}\,\overline{\mathrm{M}}$ from a DFT calculation including SOC (a) and without SOC for even (b) and odd (c) symmetry. The respective surface-projected bulk band structures are indicated by golden and yellow shaded areas. Beige (light-blue) shaded regions in (b) and (c) mark noninverted (inverted) band gaps. The dots in (a)–(c) indicate the probability density of the respective states on the topmost three Re layers. (d) TB model without SOC. (e) Band structure of the TB model including SOC with contributions of the Tamm $\psi_t^{\uparrow}$ (dark-green), $\psi_t^{\downarrow}$ (light-green) and Shockley $\psi_s^{\uparrow}$ (light-red), $\psi_s^{\downarrow}$ (orange) states. (f) Spin-up (spin-down) character of the bands is indicated by red (blue) dots. Bands which are resonant to bulk states are denoted by light-red and light-blue dots.

surface state in the band gap with $|k_{\parallel}| \geqslant 0.33$ Å^{-1} [light-blue region in Fig. 2(c)]. In the calculation for the *ideal* surface (see Supplemental Material), it is only slightly shifted in energy by about 20 meV. Moreover, this gap has an inverted structure (see Supplemental Material). Therefore, we denote this state as Shockley-type state.

Neglecting SOC, surface-projected band gaps of crystals which have bulk inversion symmetry along the direction perpendicular to the surface are called inverted gaps if they are formed by bulk bands that have exchanged parity [6,12]. Bulk Re has mirror symmetry along ⟨0001⟩, i.e., the z direction. Therefore, along $\overline{\Gamma}\,\overline{\mathrm{M}}$, the odd (with respect to x) states between -1 and 1 eV, which are formed by d_{xy} and d_{xz} orbitals, have positive and negative parity (referring to a change of the sign in the z coordinate), respectively. A $\mathbf{k}_{\parallel}$-dependent inverted gap [light-blue colored area in Fig. 2(c)] is formed by bulk states which have exchanged parity as a function of $\mathbf{k}_{\perp}$. We note that this classification of the gap for each $\mathbf{k}_{\parallel}$ is in accord with a description of the one-dimensional band topology based on the Zak phase [33,34].

For a qualitative understanding of the present hybridization effects, we present a microscopic tight-binding (TB) model which comprises the Tamm ψ_t and the Shockley ψ_s state interacting via spin-orbit coupling. In the following discussion, we restrict ourselves to wave vectors $\mathbf{k}_{\parallel}$ along the $\overline{\Gamma}\,\overline{\mathrm{M}}$ direction, i.e., along k_y. The DFT calculation without SOC shows that the even Tamm state mainly consists of s-p_z, d_{yz}, and $d_{x^2-y^2}$ orbitals located at the atoms of the surface layer. The contributions of these orbitals depend distinctly on $k = k_y$. The explicit composition of the state and further details of the model are given in the Supplemental Material [32]. The dispersion of the Tamm state is approximately

$$E_t(k) = E_{0t} + V[\cos(kb) - 1] \tag{1}$$

with $E_{0t} = 0.64$ eV, $V = 0.57$ eV, and $b = 7.5$ Å as inferred from the DFT result [see Fig. 2(a)]. For small wave vectors, the odd Shockley state basically consists of d_{xy} orbitals. At larger k values, there is an admixture of d_{xz} orbitals. The Shockley state has an almost quadratic dispersion described by

$$E_s(k) = E_{0s} + V'k^2 \tag{2}$$

with $E_{0s} = -0.76$ eV and $V' = 3.8$ eV Å^2. Figure 2(d) shows the k-dependent energies of the Tamm and the Shockley state. Dashed lines are used in the regions of $\mathbf{k}$ space, in which these states energetically overlap with Re bulk energies. The spin-orbit coupling between the d orbitals is taken into account within the on-site approximation [35] employing the strength $\lambda = 0.175$ eV of SOC in a Re atom.

Figures 2(d) and 2(e) show the eigenvalues of the (4×4) Hamilton matrix without and with SOC, respectively. The original Tamm and Shockley states are twofold degenerate with respect to spin up and spin down. Under the influence of SOC, a gap opening is observed between the states. The two energetically higher bands (W_1, W_2) have a dispersion with double W shape which nicely agrees with the result of the DFT calculation as well as with the experimental findings. W_1 results from a coupling between the Tamm spin-up state $\psi_t^{\uparrow}$ and the Shockley spin-down state $\psi_s^{\downarrow}$. For small k values, W_1 has mainly contributions from $\psi_t^{\uparrow}$ while the portions of $\psi_s^{\downarrow}$ dominate for large wave vectors. Accordingly, we observe the spin expectation value to be $\uparrow$ for small k and $\downarrow$ for large k [see Fig. 2(f)]. The coupling between $\psi_t^{\downarrow}$ and $\psi_s^{\uparrow}$ gives rise to the band W_2 with a composition analog to W_1 but interchanged spin orientations. The bands W_1' and W_2' are the counterparts of W_1 and W_2, respectively, with permuted contributions of Tamm and Shockley states.

According to Fig. 2(e), we expect γ to have predominantly odd symmetry with only small admixture of even symmetry. Therefore, it should be hardly visible in ARPES with p-polarized light. This is supported by our data in Fig. 1(c), where γ appears with small intensity along $\overline{\Gamma}\,\overline{\mathrm{M}}$, while it has larger intensity along $\overline{\Gamma}\,\overline{\mathrm{K}}$ (no mirror-plane symmetry).

We have calculated the layer-dependent probability density $|\psi|^2$ for the α, β, and γ branches of the surface state (layer 1

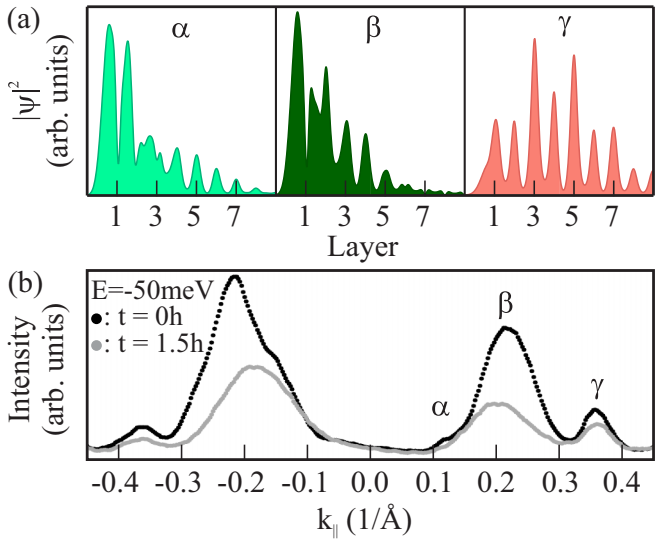

FIG. 3. (a) Layer-dependent probability density $|\psi|^2$ of the three branches of the surface state [same colors as in Fig. 2(e)]. (b) Experimental MDCs along $\overline{\Gamma}\,\overline{\mathrm{M}}$ for the pristine (aged) surface as black (gray) dots.

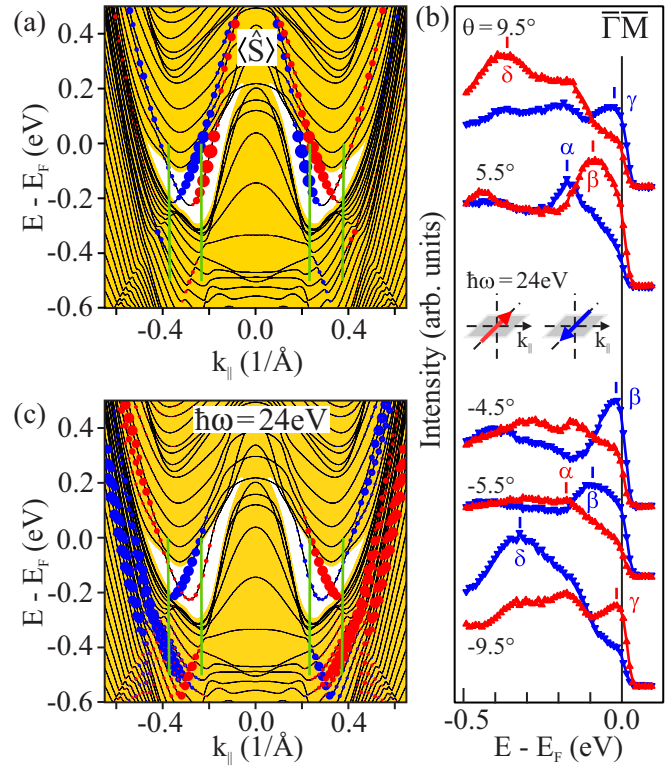

FIG. 4. (a) DFT calculation of the Re(0001) surface along $\overline{\Gamma}\,\overline{\mathrm{M}}$. Red (blue) dots indicate the intrinsic spin expectation value (Rashba component) for spin-up (spin-down) electrons of the surface states. (b) Experimental spin-resolved energy distribution curves (EDCs) for *p*-polarized light with $\hbar\omega = 24$ eV for selected electron emission angles θ. (c) Calculations including matrix elements with free-electron-like final states to model SARPES results with $\hbar\omega = 24$ eV. The dot size is a measure of the expected spectral intensity. The approximate "paths" of the energy distribution curves within the $E(\mathbf{k}_\parallel)$ plot are marked by green lines in (a) and (c).

represents the topmost layer), as shown in Fig. 3(a). While the electrons of α and β are predominantly localized in the first three layers, the situation is qualitatively different for γ with the probability density rather being extended over seven layers with maximum charge at layers three to five. Is there any experimental access to distinguish between Shockley and Tamm character of a surface state? Since Tamm states only exist at the *real* surface, while Shockley states also appear at the *ideal* surface, we expect that Tamm states are more sensitive to adsorption processes.

We put this prediction to an experimental test by comparing the ARPES data of the pristine surface with data after having exposed the sample to residual gases in UHV for 1.5 hours. Due to adsorbates, surface-related spectral features may get quenched in intensity and possibly shifted in energy. This behavior is found in our measurements. Momentum distribution curves (MDCs) along the $\overline{\Gamma}\,\overline{\mathrm{M}}$ direction at a constant energy of $E - E_\mathrm{F} = -50$ meV are displayed in Fig. 3(b). While for β the spectral intensity is reduced to about 43%, γ retains approximately 72% of its intensity upon residual-gas adsorption. This behavior is attributed to the different character of Tamm- and Shockley-type states. Note that no information can be gained from α due to its overall small intensity.

In addition to the SOC-induced mixing of Tamm and Shockley states, SOC is predicted to lift the spin degeneracy of the surface states, as already shown in Fig. 2(f). This is confirmed by our DFT calculations shown in Fig. 4(a). The sizes of the red and blue dots denote the intrinsic spin expectation values (Rashba component) of the surface-state branches: blue (α), red (β and γ) for positive $k_\parallel$ values and reversed for negative $k_\parallel$ values. Our SARPES data for $\theta \approx +5$ and -5° prove the expected opposite spin character of the α and β branches as well as their reversal upon a sign change in θ [see Fig. 4(b)]. In contrast, the spin polarization of γ is opposite to the prediction of the intrinsic spin polarization. Considering the transition matrix element including initial and final states changes the expected spin polarization for γ but not for α and β as presented in Fig. 4(c). This is one more example that the spin polarization detected by SARPES does not always reflect the intrinsic spin polarization of the initial state in the presence of mixed orbital symmetries [36–39].

In conclusion, we revealed the origin of a double W-shaped surface band on Re(0001). Its $E(\mathbf{k}_\parallel)$ dispersion and spin texture is traced back to a spin-orbit-induced mixing of a Tamm- and a Shockley-type surface state, which appear in two different gaps of the surface-projected bulk band structure. We developed criteria for theory and experiment to distinguish between the two paradigmatic surface-state types: type of gap, behavior at *real* and *ideal* surfaces, layer-dependent charge densities, and sensitivity to surface contamination. By means of high-resolution SARPES experiments, TB model calculations, as well as DFT calculations including the photoemission process, we provide a consistent picture of the role of SOC for the interplay between different types of surface states.

M.D., P.J.G., and M.H. gratefully acknowledge the hospitality of the Hiroshima Synchrotron Radiation Center and the excellent experimental support. (S)ARPES measurements

were performed with the approval of the HiSOR program advisory committee (Proposals No. 19BG026 and No. 20AU006). This work was supported by JSPS KAKENHI Grants No. 16H02114, No. 18H01954, and No. 20H00347. We thank N-BARD, Hiroshima University, for supplying the liquid helium. We are indebted to J. Braun, J. Minár, S. Schemmelmann, F. Schöttke, and E. F. Schwier for helpful discussions.

[1] S. D. Kevan, *Angle-Resolved Photoemission: Theory and Current Applications*, Studies in Surface Science and Catalysis Vol. 74 (Elsevier, Amsterdam, 1992).

[2] F. Forstmann, The concepts of surface states, Prog. Surf. Sci. **42**, 21 (1993).

[3] M. Stęślicka, From Tamm to Shockley: An historical comment, Prog. Surf. Sci. **42**, 11 (1993).

[4] A. Goldmann and R. Matzdorf, Surface states on metals, in *Surface Science*, edited by R. J. MacDonald, E. C. Taglauer, and K. R. Wandelt (Springer, Berlin, Heidelberg, 1996), p. 51.

[5] H. Lüth, *Solid Surfaces, Interfaces and Thin Films*, 5th ed. (Springer, New York, 2010).

[6] R. M. Martin, *Electronic Structure* (Cambridge University Press, Cambridge, UK, 2020).

[7] J. Kłos, Conditions of Tamm and Shockley state existence in chains of resonant cavities in a photonic crystal, Phys. Rev. B **76**, 165125 (2007).

[8] N. Malkova and C. Z. Ning, Interplay between Tamm-like and Shockley-like surface states in photonic crystals, Phys. Rev. B **76**, 045305 (2007).

[9] N. Malkova, I. Hromada, X. Wang, G. Bryant, and Z. Chen, Transition between Tamm-like and Shockley-like surface states in optically induced photonic superlattices, Phys. Rev. A **80**, 043806 (2009).

[10] N. Korozlu, O. A. Kaya, A. Cicek, and B. Ulug, Acoustic Tamm states of three-dimensional solid-fluid phononic crystals, J. Acoust. Soc. Am. **143**, 756 (2018).

[11] I. Tamm, Über eine mögliche Art der Elektronenbindung an Kristalloberflächen, Z. Physik **76**, 849 (1932).

[12] W. Shockley, On the surface states associated with a periodic potential, Phys. Rev. **56**, 317 (1939).

[13] J. Zak, Symmetry criterion for surface states in solids, Phys. Rev. B **32**, 2218 (1985).

[14] In our DFT calculation employing a basis set of localized orbitals, the ideal surface is characterized by a Hamiltonian matrix with the same elements at the surface as in the interior of the slab.

[15] J. Kłos and H. Puszkarski, Conditions of coexistence of Tamm and Shockley states in a superlattice with a perturbed surface, Phys. Rev. B **68**, 045316 (2003).

[16] *Polarized Electrons in Surface Physics*, edited by R. Feder (World Scientific, Singapore, 1985).

[17] M. Donath, Spin-dependent electronic structure at magnetic surfaces: The low-Miller-index surfaces of nickel, Surf. Sci. Rep. **20**, 251 (1994).

[18] P. D. Johnson, Spin-polarized photoemission, Rep. Prog. Phys. **60**, 1217 (1997).

[19] Y. A. Bychkov and E. I. Rashba, Properties of a 2D electron gas with lifted spectral degeneracy, JETP Lett. **39**, 78 (1984).

[20] U. Heinzmann and J. H. Dil, Spin–orbit-induced photoelectron spin polarization in angle-resolved photoemission from both atomic and condensed matter targets, J. Phys.: Condens. Matter **24**, 173001 (2012).

[21] T. Okuda and A. Kimura, Spin- and angle-resolved photoemission of strongly spin–orbit coupled systems, J. Phys. Soc. Jpn. **82**, 021002 (2013).

[22] S. Ouazi, T. Pohlmann, A. Kubetzka, K. von Bergmann, and R. Wiesendanger, Scanning tunneling microscopy study of Fe, Co and Cr growth on Re(0001), Surf. Sci. **630**, 280 (2014).

[23] A. Urru and A. Dal Corso, Spin-polarized electronic surface states of Re(0001): An ab-initio investigation, Surf. Sci. **686**, 22 (2019).

[24] H. J. Elmers, J. Regel, T. Mashoff, J. Braun, S. Babenkov, S. Chernov, O. Fedchenko, K. Medjanik, D. Vasilyev, J. Minar, H. Ebert, and G. Schönhense, Rashba splitting of the Tamm surface state on Re(0001) observed by spin-resolved photoemission and scanning tunneling spectroscopy, Phys. Rev. Research **2**, 013296 (2020).

[25] J. Regel, T. Mashoff, and H. J. Elmers, Quasiparticle interference of spin momentum locked surface states at step edges on Re(0001), Phys. Rev. B **102**, 115404 (2020).

[26] S. Schemmelmann, P. Krüger, F. Schöttke, and M. Donath, Rashba-split surface state and spin-dependent photon emission from Re(0001) at $\overline{\Gamma}$, Phys. Rev. B **104**, 205425 (2021).

[27] T. Okuda, K. Miyamaoto, H. Miyahara, K. Kuroda, A. Kimura, H. Namatame, and M. Taniguchi, Efficient spin resolved spectroscopy observation machine at Hiroshima Synchrotron Radiation Center, Rev. Sci. Instrum. **82**, 103302 (2011).

[28] R. D. Diehl, J. Ledieu, N. Ferralis, A. W. Szmodis, and R. McGrath, Low-energy electron diffraction from quasicrystal surfaces, J. Phys.: Condens. Matter **15**, R63 (2003).

[29] J. P. Perdew and A. Zunger, Self-interaction correction to density-functional approximations for many-electron systems, Phys. Rev. B **23**, 5048 (1981).

[30] B. Stärk, P. Krüger, and J. Pollmann, Magnetic anisotropy of thin Co and Ni films on diamond surfaces, Phys. Rev. B **84**, 195316 (2011).

[31] L. A. Hemstreet, C. Y. Fong, and J. S. Nelson, First-principles calculations of spin-orbit splittings in solids using nonlocal separable pseudopotentials, Phys. Rev. B **47**, 4238 (1993).

[32] See Supplemental Material at http://link.aps.org/supplemental/10.1103/PhysRevB.105.L241412 for further details of the tight-binding model.

[33] J. Zak, Berry's Phase for Energy Bands in Solids, Phys. Rev. Lett. **62**, 2747 (1989).

[34] G. van Miert, C. Ortix, and C. M. Smith, Topological origin of edge states in two-dimensional inversion-symmetric insulators and semimetals, 2D Mater. **4**, 015023 (2016).

[35] M. D. Jones and R. C. Albers, Spin-orbit coupling in an f-electron tight-binding model: Electronic properties of Th, U, and Pu, Phys. Rev. B **79**, 045107 (2009).

[36] C. Jozwiak, Y. L. Chen, A. V. Fedorov, J. G. Analytis, C. R. Rotundu, A. K. Schmid, J. D. Denlinger, Y.-D. Chuang, D.-H. Lee, I. R. Fisher, R. J. Birgeneau, Z.-X. Shen, Z. Hussain, and A. Lanzara, Widespread spin polarization effects in photoemission from topological insulators, Phys. Rev. B **84**, 165113 (2011).

[37] S. N. P. Wissing, A. B. Schmidt, H. Mirhosseini, J. Henk, C. R. Ast, and M. Donath, Ambiguity of Experimental Spin Information from States with Mixed Orbital Symmetries, Phys. Rev. Lett. **113**, 116402 (2014).

[38] H. Wortelen, H. Mirhosseini, K. Miyamoto, A. B. Schmidt, J. Henk, and M. Donath, Tuning the spin signal from a highly symmetric unpolarized electronic state, Phys. Rev. B **91**, 115420 (2015).

[39] H. Maaß, H. Bentmann, C. Seibel, C. Tusche, S. V. Eremeev, T. R. F. Peixoto, O. E. Tereshchenko, K. A. Kokh, E. V. Chulkov, J. Kirschner, and F. Reinert, Spin-texture inversion in the giant Rashba semiconductor BiTeI, Nat. Commun. **7**, 11621 (2016).